American Mineralogist, Volume 63, pages 350–364, 1978

The system Mg_2SiO_4–Fe_2SiO_4–$CaAl_2Si_2O_8$–SiO_2 and the origin of Fra Mauro basalts

BRUCE R. LIPIN

U.S. Geological Survey, 954 National Center
Reston, Virginia 22092

Abstract

Equilibrium relations of mixtures in the $(Mg_{0.59}Fe_{0.41})_2SiO_4$–$CaAl_2Si_2O_8$–$SiO_2$ plane reveal a liquidus surface similar to that found by Andersen (1915) in the iron-free portion of the system. Three piercing points were determined: at 1270 ± 5°C liquid, olivine, anorthite and spinel are in equilibrium; at 1218 ± 5°C liquid, olivine, orthopyroxene, and anorthite are in equilibrium; and at 1186 ± 5°C liquid, orthopyroxene, anorthite, and silica are in equilibrium. Iron–magnesium partition coefficients between solid and liquid phases [$K_D = (X\text{Fe})_{xtal}(X\text{Mg})_{liq}/(X\text{Mg})_{xtal}(X\text{Fe})_{liq}$] are 0.30 (1250–1170°C) for orthopyroxene, 0.33 (1270–1180°C) for olivine, and 0.41 for spinel at 1272°C.

Liquidus–solidus phase relations, especially in the vicinity of the olivine–anorthite–orthopyroxene–liquid equilibrium, are, however, very different from the iron-free portion of the system. The three crystalline phases coexist with a liquid over a wide range of temperatures and liquid compositions [30°C, Fe/(Fe + Mg) between 0.41 and 0.60]. Thus it is possible for lunar Fra Mauro basalts, with compositions close to those of the triply-saturated liquids, to represent residual liquids of a lunar-wide magma ocean. Evidence from rare-earth element abundances and isotope systematics are found to be compatible with a residual-liquid origin for Fra Mauro basalts.

Introduction

Lunar highland rocks are included in samples returned from all Apollo and Luna missions. Although these rocks vary widely with regard to texture and mineralogy, Walker *et al.* (1972, 1973) recognized that the lunar highland rocks, including Fra Mauro basalts, are compositionally defined by the system $CaAl_2Si_2O_8$–Mg_2SiO_4–Fe_2SiO_4–SiO_2 and that their compositional trends can be most adequately explained by low-pressure, low-fO_2 crystal-liquid equilibrium processes. Most petrologists view the highland rocks as originally the products of igneous processes (*e.g.* Prinz *et al.*, 1973; Roedder and Weiblen, 1972), that underwent extensive textural alteration due to impacts or annealing or both.

Phase-equilibrium studies of natural lunar highland samples have been carried out by Walker *et al.* (1972, 1973), who constructed boundary curves on an olivine–anorthite–silica plane on the basis of those experiments. However, partly because of the variability of the bulk composition of natural samples, their diagram is not at constant Fe/(Fe + Mg). The strategy employed in the present investigation was to study phase relations in the pure system Mg_2SiO_4–Fe_2SiO_4–$CaAl_2Si_2O_8$–SiO_2 in order to determine if phase relations in this system do indeed closely approximate those determined by Walker *et al.* for the highland rocks, and to accurately determine liquidus–solidus phase relations to complement the earlier work. Inasmuch as the system Mg_2SiO_4–$CaAl_2Si_2O_8$–SiO_2 had previously been investigated by Andersen (1915), a plane of intermediate Fe/Mg ratio [atomic Fe/(Fe + Mg) = 0.41] hereafter called the iron-41 plane (Fig. 1) was investigated. This Fe/(Fe + Mg) ratio is close to the average for many lunar highland rock types (see for example Taylor, 1975, p. 232–234).

The experimental results are applied to the problem of the origin of the Fra Mauro basalts. The conclusion reached is that Fra Mauro basalts are more probably residual liquids of a lunar-wide magma than partial melts from the interior. Some of the arguments are based upon the experimental results of this study and phase-equilibrium considerations, while others are based upon a generally accepted model of lunar evolution and are, of course,

0003-004X/78/0304-0350$02.00

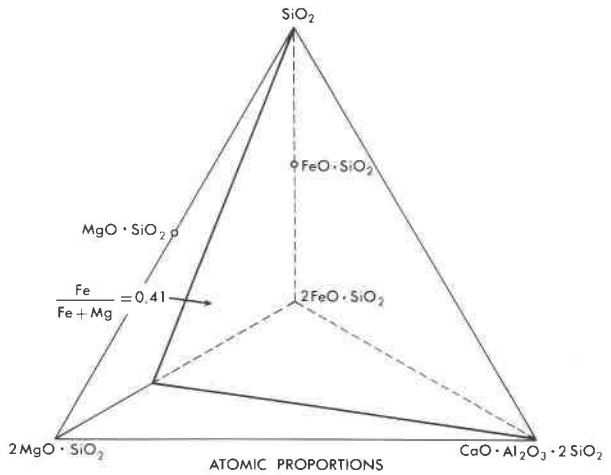

Fig. 1. The Mg_2SiO_4–$CaAl_2Si_2O_8$–Fe_2SiO_4 tetrahedron and the position of the iron-41 plane.

dependent upon that model. Arguments of the latter kind are labeled as such.

Experimental method

Weighed mixtures of reagent-grade chemicals were fused in air. The glass was then crushed to 100 mesh, placed in 70% Ag–30% Pd containers, and heated to 1000°C for 8 hours in a 1:1 CO_2/H_2 mixture ($fO_2 \simeq 10^{-14.5}$ atm) following the method described by Muan and Schairer (1971). The crystalline, pre-reduced mixtures containing anorthite + pyroxene ± olivine were then placed in high-purity iron crucibles and sealed in evacuated silica tubes for final equilibration. Temperatures in the vertical quench furnaces were measured with a Pt/90Pt-10Rh thermocouple calibrated against the melting points of Au (1064.43°C) and $CaMgSi_2O_6$ (1395.3°C). Run products were identified with a reflected and transmitted light microscope, and individual phases were analyzed with an

Table 1. Results of critical runs in the system $(Mg_{0.59}Fe_{0.41})_2SiO_4$–$CaAl_2Si_2O_8$–$SiO_2$

Bulk Composition (Mol%)						
Fe/(Fe+Mg)	Ol	An	SiO_2	T(°C)	Duration (hours)	Phases[#]
.416	38	33	29	1272	66	l+sp(tr)[##]
				1264	23½	l+an+ol(tr)+sp(tr)
				1257	23½	l+an+ol
				1203	47	an+ol+l
				1170	113	an+opx+ol
.426	32	31	37	1304*	2-64	l
				1272	24	l+an
				1242	45	l+an
				1229	45	l+an+ol
				1206*	2-64	l+an+ol
				1187	24	an+opx+l+ol
				1168	40½	an+opx+ol(tr)**
.406	30	27	43	1273	42½	l
				1250	26½	l+an(tr)
				1234	161	l+an+ol
				1223	44½	l+an+ol+opx(tr)
				1211	26½	l+an+ol+opx
				1198	44½	an+opx+l+ol
				1187	42½	an+opx+ol(tr)+l(tr)
.389	32	24	44	1255	24	l
				1244	18	l+ol(tr)
				1223	65	l+ol
				1214	64½	l+an+ol+opx
				1209	24	l+an+opx+ol
				1198	65	opx+an+l+ol
				1180	71	opx+an+l+ol
				1167	113	an+opx+si(tr)

Bulk Composition (Mol%)						
Fe/(Fe+Mg)	Ol	An	SiO_2	T(°C)	Duration (hours)	Phases
.416	26	21	53	1232	21	l
				1212	21	l+opx
				1199	21½	l+opx
				1194	70	l+opx+an
				1187	70	l+opx+an
				1177	48	opx+an+l(tr)
.406	23	17	60	1248	17½	l
				1221	41	l+opx
				1198	41	l+opx+si
				1188	41	l+opx+si+an(tr)
				1181	89½	l+opx+si+an
				1177	69	an+opx+si+l
				1162	137½	opx+an+si
.425	18	18	64	1124	22	l
				1203	25½	l+opx(tr)
				1189	1-112+	l+opx+si
				1181	112	l+opx+an+si
				1175	87½-112+	l+an+opx+si
				1173	70	l+an+opx+si
				1163	87½-65½+	an+opx+si+l(?)
				1158	70	an+opx+si

Temperatures and Liquid Compositions at the Three Piercing Points in the Iron 41 Plane

39	31	30	1270±5°C	-- l+an+ol+sp
29	22	49	1218±5°C	-- l+an+opx+ol
17	19	64	1186±5°C	-- l+an+opx+si

[#] Abbreviations are as follows: l = liquid, sp = spinel, ol = olivine, opx = orthopyroxene, an = anorthite, si = silica, (tr) = trace amount.

[##] For each run, phases are listed in order of abundance.

* These temperatures were run at 2, 17, 40, and 64 hrs. in order to check equilibrium.

** Only a few, badly embayed grains of olivine remaining.

\+ The first number denotes the duration of a conventional run. The second number is the time another charge of the same composition was held at the same temperature after being cooled at 3°/hr. from above the liquidus.

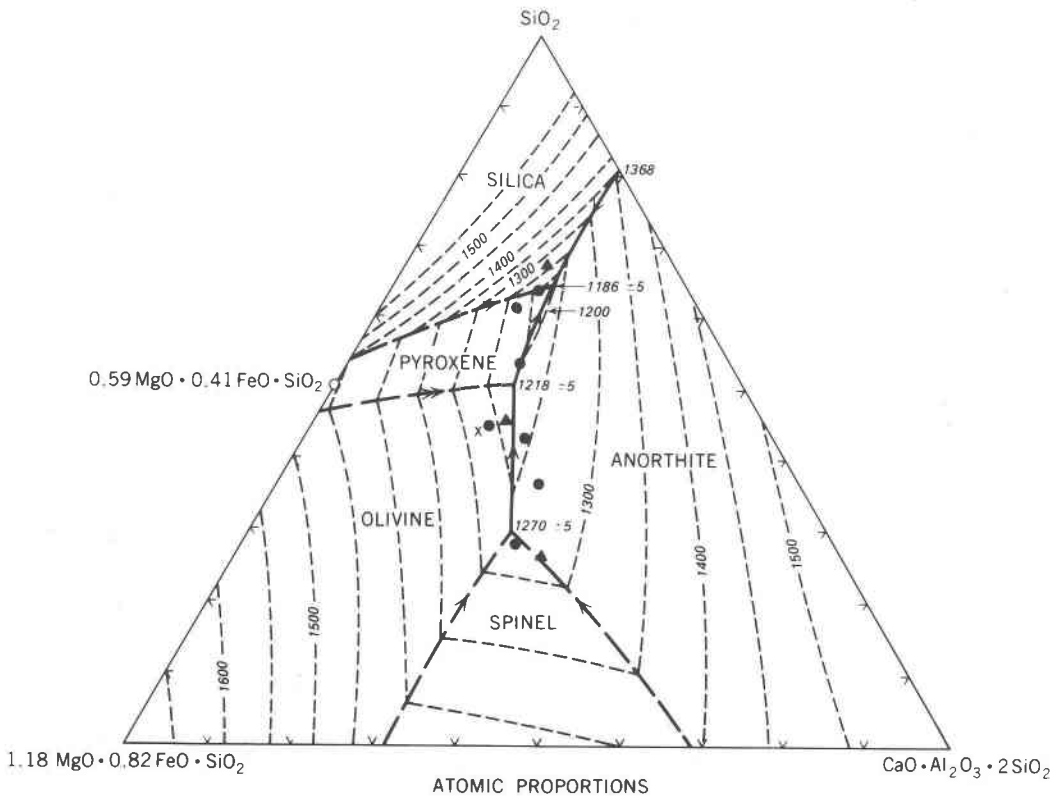

Fig. 2. The liquidus surface of the iron-41 plane. The position of the pyroxene boundaries at the olivine–silica edge are from the data of Bowen and Schairer (1935). The dots represent bulk compositions studied. The triangles are piercing-point compositions found by Walker *et al.* (1972) in the natural system. The equilibrium crystallization of liquid *X* is discussed in the text. Although only orthopyroxene was encountered, the appropriate field is labelled "pyroxene" because the "proto" form might be stable at higher temperatures. For positions of the three piercing points see Table 1.

automated ARL-SEM electron microprobe operating at 15 kV and 0.05 μm sample current. The data were processed by the Bence-Albee method using Kakanui garnet (B. Mason, donor), glass CG77135 (J. Minkin, donor), and Adirondack diopside (U.S. National Museum #117733, W. Melson, donor) as standards. Periodic test analyses were performed on these phases. As a check on bulk composition, each mixture was brought to a temperature above its liquidus for at least 24 hours and the resultant glass was analyzed. The small increase (0.03–0.06) in Fe/(Fe + Mg) of the mixtures over their calculated values can be accounted for by reaction of the small amount of remaining Fe^{3+} with the iron crucibles. The final bulk compositions in terms of olivine, anorthite, silica, and Fe/(Fe + Mg) of the mixtures from the microprobe analyses are reported in Table 1. By varying lengths of runs, approaching a specific temperature from both directions, estimating proportions of phases optically, and analyzing the run products with the electron microprobe, it was found that in most cases a close approach to equilibrium was reached in 2–6 hours. However, no reported run was less than 17 hours. For runs near the solidus no run was less than 48 hours.

Results

The results of the experiments are given in Table 1, which includes temperatures and compositions of the three piercing points. The results are summarized graphically in Figure 2, which shows the liquidus surface of the iron-41 plane. Note the locations of the boundary curves at the $(Mg_{0.59}Fe_{0.41})_2SiO_4$–$SiO_2$ edge (Fig. 2). The orthopyroxene composition is within its primary field at bulk Fe/(Fe + Mg) values between 0.15 and 0.54 in the system MgO–FeO–SiO_2 (Bowen and Schairer, 1935). However, olivine is still in reaction relation with the liquid along most of the olivine–orthopyroxene boundary curve (see Bowen and Schairer, 1935, p. 187). Some recent studies have the pyroxene boundary curves incorrectly placed. Electron microprobe analyses of coexisting phases near

Table 2. Electron microprobe analyses of coexisting ferromagnesian phases in the system anorthite–olivine–silica

	l-ol-sp-an††			l-ol-opx-an			l-opx-an-si		l*
T(°C)	1264			1214			1181		1189
				Weight Percent Oxides					
Phase	l	ol	sp	l	ol	opx	l	opx	l
SiO_2	45.1	39.5	0.26	51.1	38.7	56.1	56.9	55.6	50.1
	(1.04)**	(.552)	(.051)	(.466)	(1.16)	(2.61)	(.441)	(1.30)	(.963)
Al_2O_3	18.16	0.12	67.6	15.70	0.05	1.49	15.53	1.99	14.73
	(.503)	(.045)	(1.86)	(.249)	(.015)	(.634)	(.219)	(.374)	(.461)
MgO	11.09	43.2	20.6	9.56	42.0	29.7	6.73	29.4	7.26
	(.272)	(1.27)	(.325)	(.415)	(.348)	(.269)	(.209)	(.202)	(.216)
FeO	14.34	18.21	12.00	13.78	20.05	12.34	10.45	13.29	17.79
	(.463)	(.010)	(.985)	(.913)	(.021)	(.322)	(.633)	(.288)	(.283)
CaO	10.37	0.35	0.07	9.95	0.29	1.13	8.59	0.87	8.39
	(.252)	(.056)	(.011)	(.045)	(.064)	(.344)	(.070)	(.050)	(.190)
Total	99.06	101.38	100.53	100.09	101.09	100.76	98.20	101.15	98.27
				Cation Totals					
Si	1.670	0.991	0.005	1.842	0.984	1.970	2.017	1.957	1.868
Al	0.792	0.003	1.982	0.666	0.000	0.061	0.648	0.083	0.647
Mg	0.612	1.619	0.763	0.513	1.593	1.558	0.355	1.540	0.403
Fe	0.443	0.382	0.250	0.414	0.426	0.362	0.309	0.390	0.555
Ca	0.411	0.009	0.001	0.384	0.000	0.042	0.326	0.030	0.335
Total	3.928	3.004	3.001	3.819	3.003	3.993	3.655	4.000	3.808
Oxygens	6	4	4	6	4	6	6	6	6
$\frac{Fe}{Fe+Mg}$	0.419	0.190	0.247	0.446	0.216	0.192	0.465	0.202	0.579

† *All compositions are averages of 2 or 3 analyses.*
†† *Abbreviations as in Table 1.*
* *An iron-rich liquid in equilibrium with an, ol, and opx on the (si) curve at about point A in Figure 4.*
** *Standard Deviation (2σ).*

the piercing points are given in Table 2 and shown in Figure 3. The temperatures of the three piercing points are, as expected, lower than those found by Andersen (1915) in the iron-free system, and the composition of the liquid at the piercing points has shifted toward the $(Mg,Fe)_2SiO_4$–SiO_2 edge.

Although the system is not strictly quaternary, partly due to the existence of spinel, the phase relations can, to a first approximation, be represented in a tetrahedron (Fig. 4). Information on the bounding pseudoternary systems was obtained from Andersen (1915), Bowen and Schairer (1935), and Roeder and Osborn (1966).

The reaction relationship between olivine and orthopyroxene may be illustrated by the following crystallization sequence, using the information presented in Figures 2 and 4. A liquid with bulk composition X in the iron-41 plane (Fig. 2) will first precipitate olivine (1275°C), which is joined by anorthite at 1220° and orthopyroxene at 1215°C. At 1215°C the liquid composition is on the (si) or silica-absent curve, with Fe/(Fe + Mg) between 0.41 and 0.45. With continued cooling, olivine (being resorbed), orthopyroxene, and anorthite remain in equilibrium with liquid, which continually changes in composition along the (si) curve for at least 30°C and a wide range of liquid compositions [Fe/(Fe + Mg) = 0.41–0.6]. At liquid composition Fe/(Fe + Mg) $\simeq$ 0.6 (see Table 2 and point *A* in Fig. 4) olivine has completely dissolved and the liquid moves across the orthopyroxene–anorthite surface (shaded portion of Fig. 4) toward the (ol) or olivine-absent curve (point *B*, Fig. 4) where

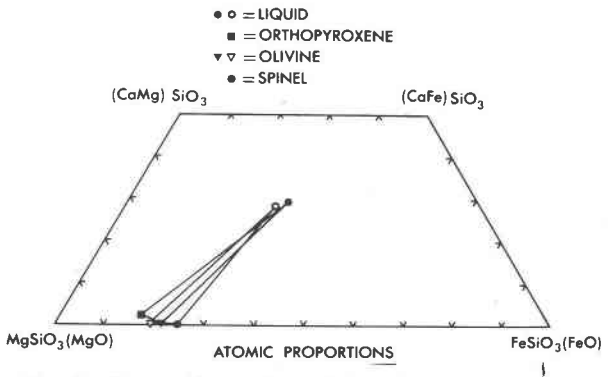

Fig. 3. Compositions of coexisting ferromagnesian phases projected onto the $CaSiO_3$–$MgSiO_3$–$FeSiO_3$ composition plane. Open symbols represent the l–ol–sp–an equilibrium and filled symbols represent the l–ol–opx–an equilibrium. Abbreviations are as in Table 1. For further explanation see text.

anorthite, orthopyroxene, and silica coprecipitate while the liquid changes composition along (ol) until the solidus (~1160°C) is reached. The solidus assemblage for all bulk compositions more SiO_2-rich than the $(Mg_{0.59}Fe_{0.41})SiO_3$–$CaAl_2Si_2O_8$ join is orthopyroxene–anorthite–silica. Hence, the five-phase element olivine–orthopyroxene–anorthite–silica–liquid is not reached during equilibrium crystallization of mixtures in the iron-41 plane.

Figure 3 shows the compositions of the coexisting phases (Table 2) projected onto the $CaSiO_3$–$MgSiO_3$–$FeSiO_3$ plane (excluding anorthite and silica). Electron microprobe analyses of the phases revealed no dependence on temperature or bulk composition of the iron–magnesium distribution coefficient; $K_D = (X\mathrm{Fe})_{xtal}(X\mathrm{Mg})_{liq}/(X\mathrm{Mg})_{xtal}(X\mathrm{Fe})_{liq}$, where $(X\mathrm{Fe})_{liq}$ = mol fraction of Fe in the liquid phase. Between 1270 and 1180°C $K_D = 0.33$ for olivine and liquid, and $K_D = 0.30$ for orthopyroxene and liquid in the range 1260–1170°C. Spinel–liquid data were not obtained over a sufficiently large range of temperatures and compositions to determine their effects on Fe–Mg partitioning between those two phases; however, at 1272°C the spinel–liquid K_D is 0.41.

The final composition of the liquid on the (ol) curve during equilibrium crystallization of composition X may be calculated with the aid of the iron–magnesium distribution coefficient between ortho-

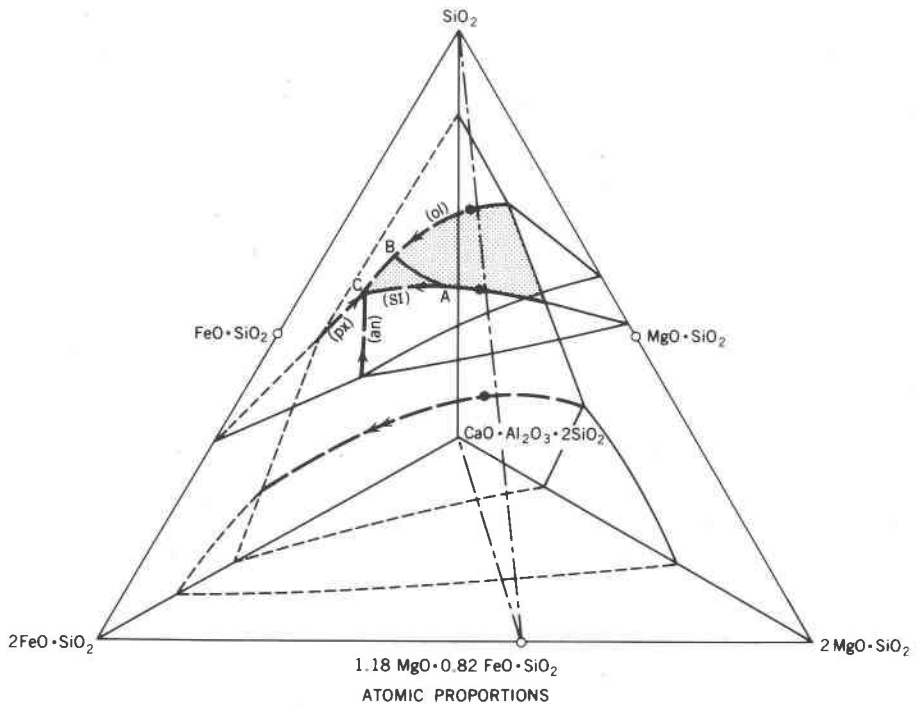

Fig. 4. Sketch of the phase relations within the Mg_2SiO_4–Fe_2SiO_4–$CaAl_2Si_2O_8$–SiO_2 tetrahedron. The medium-weight solid and dashed curves are the boundary curves in the bounding ternary systems. The heaviest curves are "univariant" curves. The unlabelled heavy, dashed curve has olivine, anorthite, and spinel in equilibrium with liquid. The other "univariant" curves leading into five-phase element (*C*) olivine–orthopyroxene–anorthite–silica–liquid are labelled with the absent phase in parentheses. The filled circles are piercing points in the iron-41 plane, which is outlined by the long and short dashed lines. The shaded area is the anorthite–orthopyroxene surface, and the curve from *A*–*B* is the approximate path across the opx–an surface taken by a liquid starting at X in Fig. 2.

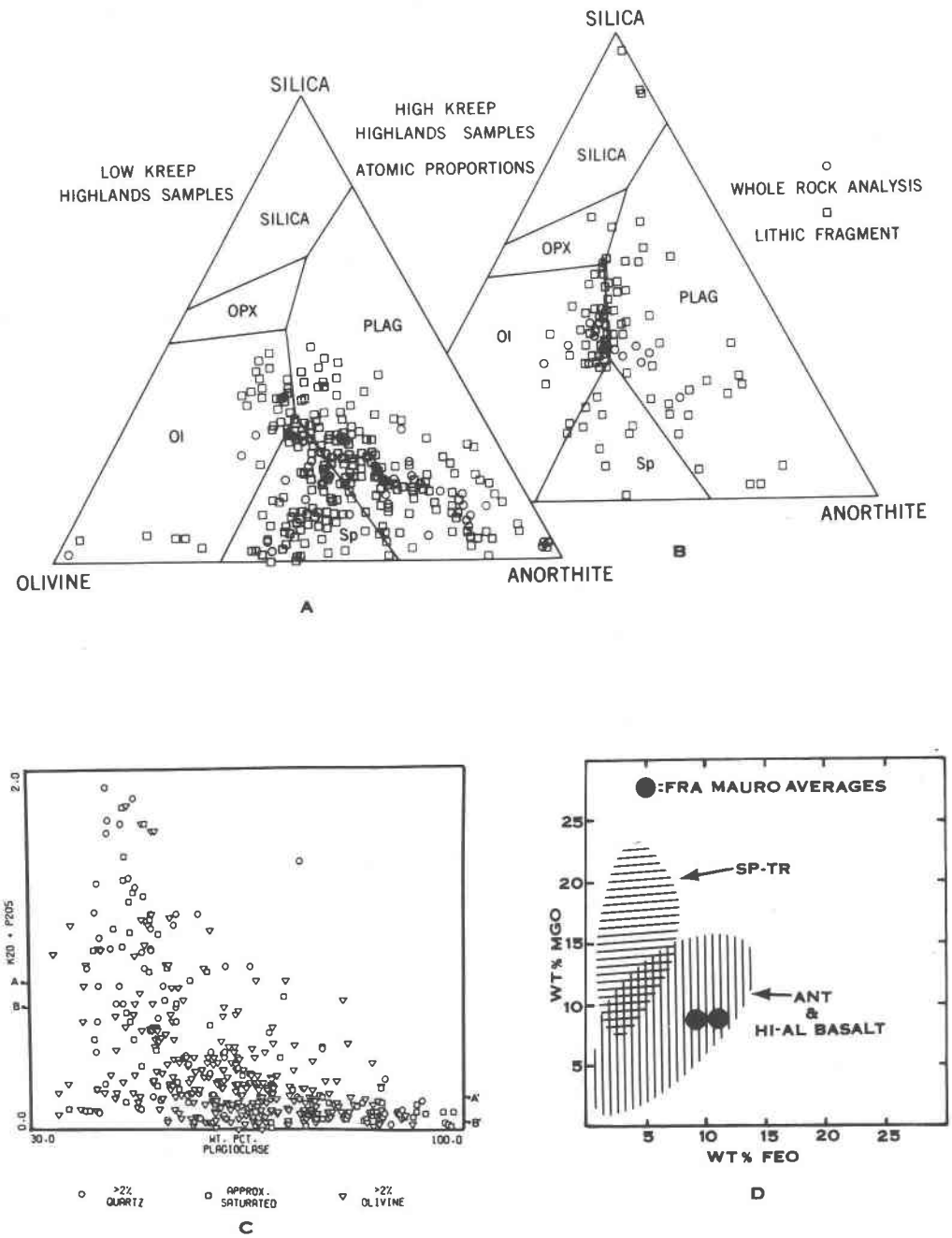

Fig. 5. Compositional relations of highland rocks and lithic fragments: (a) low-KREEP compositions (ANT, high-alumina basalts, and spinel troctolites) projected onto the iron-41 plane; (b) medium- and high-KREEP compositions (Fra Mauro basalts) projected onto the iron-41 plane; (c) $K_2O + P_2O_5$ *vs.* normative plagioclase. All compositions below *B–B′* were used in 5a, and all compositions above *A–A′* were used in 5b. Compositions between *A–A′* and *B–B′* were omitted from a and b because they represent polymict breccias; (d) FeO *vs.* MgO of highland lithic fragments from the Luna-20 site. Average FeO–MgO values for Fra Mauro basalts (Taylor, 1975) are also given. Sources: a, b, and c are from Wood (1975); d is modified from Prinz *et al.* (1973).

pyroxene and liquid, $K_D$opx–liq = (0.30). Inasmuch as orthopyroxene is the only ferromagnesian crystalline phase at the solidus of X, its Fe/(Fe + Mg) ratio must be 0.41 and the Fe/(Fe + Mg) ratio of the liquid should be approximately 0.70. Therefore, the composition with respect to the iron and magnesium of the liquid at point *C* (Fig. 4) is Fe/(Fe + Mg) > 0.70.

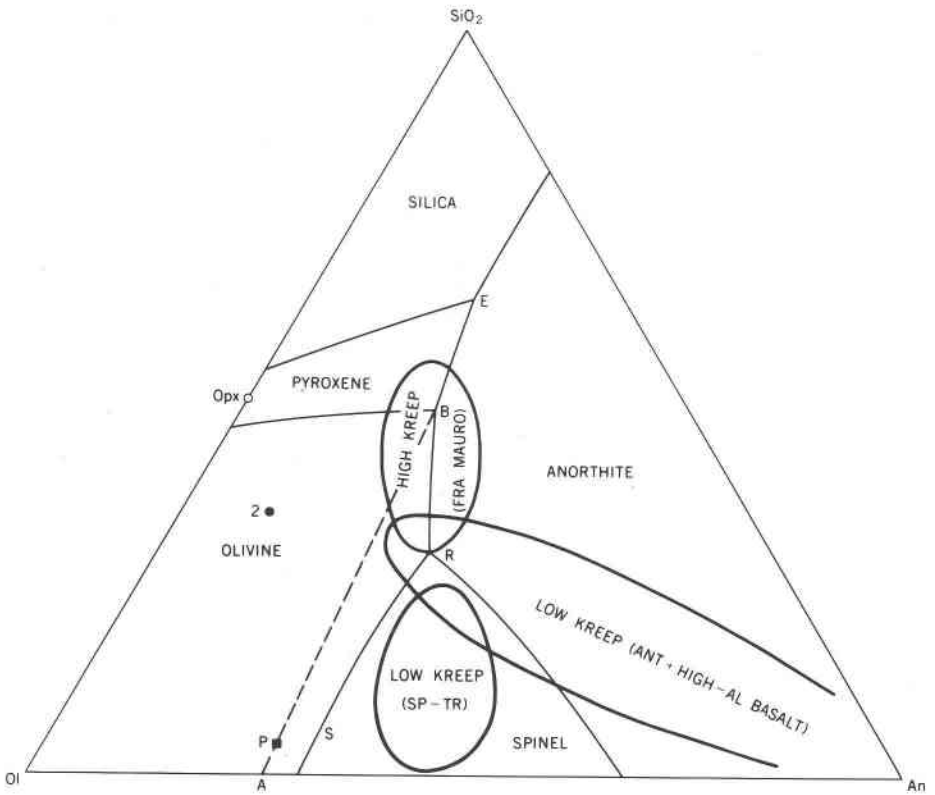

Fig. 6. High- and low-KREEP highland compositions projected onto the iron-41 plane. The high-KREEP compositions are Fra Mauro basalts. Low-KREEP samples include ANT-suite rocks, high-alumina basalts and spinel troctolites (sp–tr). Points *P* and 2 are assumed magma compositions. For further explanation see text.

Discussion

Relationship of Fra Mauro basalts to other highland rocks

A deep, fractionating magma ocean, responsible for a compositionally zoned outer moon, is a generally-accepted premise among students of lunar geology, with the most depth estimates ranging from 200 km to the radius of the moon. However, Brett (1977) has concluded that not more than the outer few hundred kilometers was originally molten. Attempts to model processes in a deep magma ocean have yielded a wide variety of ideas concerning the chemical and mineralogical makup of the outer 200–400 km (see for example Taylor and Jakeš, 1974; Hodges and Kushiro, 1974; Wood, 1975; Walker *et al.*, 1975; Ringwood, 1976; Drake, 1976). Qualitatively most of the models are similar, in that dense ferromagnesian minerals are concentrated toward the bottom of the ocean and relatively low-density plagioclase-rich cumulates are concentrated in the upper 60–100 km, with late-stage residual liquids collecting under the plagioclase-rich crust. The compositions of the plagioclase-rich cumulates, collectively known as ANT (anorthosites, norites, and troctolites), are shown in Figures 5a–d and 6. The envelope labeled ANT in Figure 6 is a continuous series ranging from anorthosite to noritic (or troctolitic) anorthosite to anorthositic norite (or troctolite) (Prinz *et al.*, 1973). The so-called low-K Fra Mauro basalts or high-alumina basalts, which loosely cluster about the olivine–anorthite–spinel point, are also included in the ANT envelope. Prinz *et al.* (1973) demonstrated that high-alumina basalts continue the major-element chemical trends exhibited by the ANT suite. Agreement on the inclusion of the high-alumina basalts in the ANT suite is not unanimous. This will be discussed below. The group of rocks called spinel troctolites (Fig. 6) is not well understood. Some investigators consider spinel troctolites to be partial melts (*e.g.* Walker *et al.*, 1973), or original cumulates (*e.g.* Prinz *et al.*, 1973), or secondary differentiates of ANT cumulates from impact melting (Wood, 1975). Whatever their origin, spinel troctolite compositions are included in

Figure 5a with ANT suite rocks and high-alumina basalts because all these samples are relatively low in KREEP (potassium, rare-earth elements, and phosphorus) compared to Fra Mauro basalts.

Figure 5b shows the compositions of the medium- and high-K Fra Mauro (or KREEP) basalts, hereafter called Fra Mauro basalts,[1] projected onto the iron-41 plane. As seen in Figure 5b and demonstrated by Walker *et al.* (1972), the Fra Mauro basalt compositions seem to cluster about the liquidus boundary curves in the iron-41 plane. Walker *et al.* (1973) also pointed out several studies in which average lithic fragment and glass compositions cluster about the ol–opx–an point and the anorthite-saturated boundary curves. The close relationship of the Fra Mauro basalt compositions with the plagioclase-saturated boundary curves emanating from the ol–opx–an point in Figures 5b and 6 suggests that the basalts represent liquid compositions rather than cumulates.

Because the Fra Mauro basalt compositions correspond to low-pressure liquidus boundary curves (0–5 kbar), Walker *et al.* (1972, 1973) concluded that their maximum depth of origin is 100 km. This depth estimate places the source region within the cumulates of the magma ocean. Fra Mauro basalts could then be the result of partial melting of some cumulate of the magma ocean or residual liquid of that ocean. The very high concentration of incompatible elements indicates that either a small amount of partial melting of the cumulates or a large amount of liquid fractionation took place.

Fractional partial melting

The Fe/(Fe + Mg) values for Fra Mauro basalts range from about 0.35 to 0.6 (Hubbard *et al.*, 1972; Reid *et al.*, 1972b), and KREEP and other incompatible elements are greatly enriched compared to other highland rock types.

Fractional (non-equilibrium) partial melting, which is continuous removal of liquid from its source, was advocated by Walker *et al.* (1973) for the production of Fra Mauro basalt and high-alumina basalt, which Walker *et al.* did not consider to be part of the ANT suite. Their model is as follows: A source with a bulk composition below the opx–an join, presumably within the ANT envelope (Fig. 6) will, upon heating, first yield a liquid at the (si) curve (Fig. 4). Liquid is continuously removed until one phase, in this case orthopyroxene, is exhausted. The liquids along the (si) curve would represent the Fra Mauro basalts. No more liquid would be produced until the temperature of the olivine–spinel–anorthite curve is reached. These later liquids at the ol–sp–an curve would represent the high-alumina basalts. If fractional partial melting did occur, a compositional hiatus between high-alumina basalts (the olivine–spinel–anorthite point) and Fra Mauro basalts (the olivine–orthopyroxene–anorthite point) would be expected.

Figures 5a–b clearly show that no such compositional gap exists between Fra Mauro basalt and high-alumina basalt compositions in the lithic-fragment and whole-rock compositions plotted by Wood.

A. J. Irving and R. B. Merrill (1976, written communication) point out that many of the compositions in Figure 5 are from electron microprobe analyses obtained with a defocused beam, and the analytical uncertainties, along with impact mixing, would obscure primary features and insure a continuum. J. A. Wood (1976, written communication) plotted 850 high- and low-KREEP glass compositions, most of which do not suffer from the uncertainties of a defocused beam analysis, and the same continuum exists in the glass compositions. Impacts obviously have occurred on the moon but the extent of mixing is hard to assess. Several studies (*e.g.* Hubbard *et al.*, 1972; Powell *et al.*, 1975; Wood, 1975) suggest that extensive mixing did *not* occur in the lunar highlands. It is clear, however, that there is no break in composition between the high- and low-KREEP samples in terms of olivine–anorthite–silica proportions.

Figure 5c, reproduced from Wood (1975), plots $K_2O + P_2O_5$, two distinctive Fra Mauro (KREEP) components, *vs.* weight percent plagioclase. No compositional hiatus appears when these parameters are considered. It is remarkable that so much overlap of low- and high-KREEP samples exists (Figs. 5a and b), when one considers that the compositions falling between *A–A'* and *B–B'* (Fig. 5c) were *not* included in Figures 5a and b.

Figure 5d shows the FeO–MgO variations in Luna 20 ANT and high-alumina basalts (Prinz *et al.*, 1973). The average compositions of Fra Mauro basalts (Taylor, 1975) show there cannot be a gap in terms of FeO–MgO variations between low- and high-KREEP rocks.

To summarize, no compositional gap appears between Fra Mauro basalts and the ANT suite, including high-alumina basalts. A fractional partial melting model cannot be supported on this basis.

[1] Fra Mauro basalt is a compositional term equivalent to KREEP basalt and high- or medium-K Fra Mauro basalt, and is used following the suggestion of Reid *et al.* (1972a).

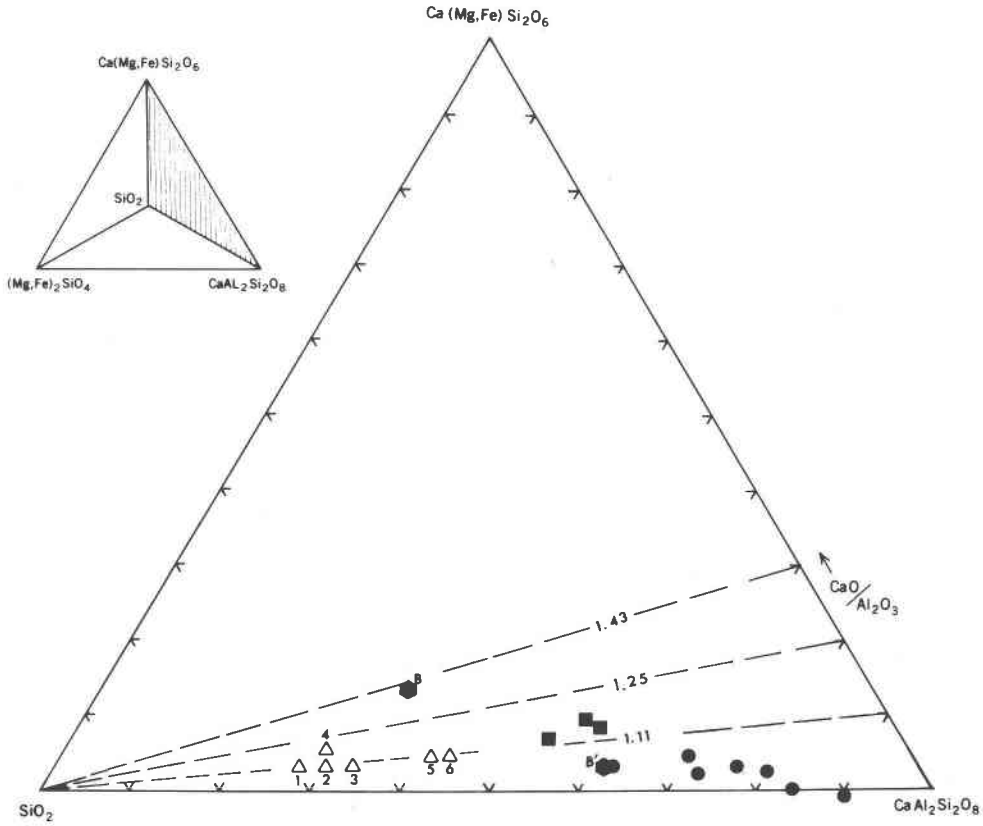

Fig. 7. Projection of average and individual highland bulk-rock compositions onto the shaded face of the tetrahedron shown in the inset. The compositions are expressed in terms of CaO/Al_2O_3 molar ratios [1.00 at the $(Mg,Fe)_2SiO_4$–$CaAl_2Si_2O_8$–SiO_2 base, and ∞ at the SiO_2–$Ca(Mg,Fe)Si_2O_6$ edge], which provide an estimate of the amount of Ca-rich clinopyroxene component in a particular composition. ANT (circles) and high-alumina basalt (squares) averages are from Prinz *et al.* (1973) and Taylor (1975). *B* = liquid composition reported by Walker *et al.* (1973) that was derived by partial melting of 60335 represented by *B'*. The following are Fra Mauro basalts: 1 = Apollo 15 high-K average (Reid *et al.*, 1972c); 2 = 14 type D average (Reid *et al.*, 1972b); 3 = 15382 (Dowty *et al.*, 1976); 4 = 15386 (Rhodes and Hubbard, 1973); 5 = Apollo 14 type C average (Reid *et al.*, 1972b); 6 = 14310 (Hubbard *et al.*, 1972).

Equilibrium partial melting

Liquids along the (si) curve (Fig. 4) which project at about point *B* (Fig. 6) have the major-element chemistry of Fra Mauro basalt. As previously stated, such liquids can be produced by partial melting of a bulk composition below the opx–an join (Fig. 6). Furthermore, equilibrium melting can produce a continuum of liquid compositions. Four sources with variable olivine, orthopyroxene, anorthite contents have been suggested:

(A) ANT suite rocks (*e.g.* Walker *et al.*, 1972);

(B) compositions near 2 in Figure 6 (Hubbard *et al.*, 1974, and Weill and McKay, 1975);

(C) very olivine-rich cumulates near composition *P* in Figure 6 with about 7× chondritic rare-earth abundances (McKay and Weill, 1976a);

(D) compositions similar to high-alumina basalts near *R* in Figure 6 (McKay and Weill, 1976b).

With respect to (A) one might ask: can ANT suite rocks melt to a Fra Mauro basalt? The answer is probably no. Figure 7 shows average and individual Fra Mauro basalt compositions from Apollo 14, 15, and 16. Fra Mauro basalts have molar CaO/Al_2O_3 ratios of 1.1 to 1.2 or about 3.5% $Ca(Mg,Fe)Si_2O_6$ component. The liquid composition Walker *et al.* (1973) quoted as representing Fra Mauro basalts (point *B*, Fig. 7) at the ol–opx–an point has CaO/Al_2O_3 = 1.38, which is nearly 14% $Ca(Mg,Fe)Si_2O_6$ component. This composition was obtained by electron microprobe analysis of a liquid derived from breccia 60335 (D. Walker, 1977, oral communication). The composition of 60335 projects at *B'* (Fig. 7) and has CaO/Al_2O_3 = 1.05, which is about average for ANT. Even if a suitably low CaO/Al_2O_3 ANT could be found, the trace-element partitioning calculations by Hubbard *et al.* (1974), Weill *et al.* (1974),

Weill and McKay (1975), and McCallum and Mathez (1975) show that plagioclase-rich compositions, such as ANT, could not simultaneously produce the trace-element and major-element characteristics of FMB. This objection also applies to case D.

With respect to (B) a composition closer to the ol–SiO_2 join than ANT with suitably low CaO/Al_2O_3 will produce liquids along the (si) curve. Composition 2 (Fig. 6), corresponding to composition 2 in Weill *et al.* (1974, p. 1342, Fig. 4) is an example. However, this bulk composition is to the olivine–silica side of *B*–ol, and once plagioclase is exhausted the liquid would follow the olivine–pyroxene boundary surface rather than olivine–anorthite surface. Such a composition is not a likely source for Fra Mauro basalts.

A very olivine-rich source could melt to (si) liquids corresponding to Fra Mauro basalts (possibility C). Further rise in temperature would result in a greater degree of melting, and the liquid composition would move up-temperature along the anorthite–olivine surface to the sp–ol–an curve. If the CaO/Al_2O_3 requirement is met, there are no phase equilibrium arguments against this kind of a source region. However, when analyzed in terms of the magma ocean hypothesis, other factors make this an unlikely source. First, for an olivine-rich cumulate such as this to have 7× chondritic REE abundances, it would have had to crystallize from a liquid with 250–350× chondritic REE abundances, depending upon which set of crystal/liquid distribution coefficients one chooses. Of course, phases in a given cumulate need not have precipitated at the same time in the crystallization history of the magma. However, if some phases carry the memory of a relatively REE-poor liquid, later additions to the cumulate must have a correspondingly larger proportion of trace elements in order for the source to have REE abundances 7× those of chondrites. In other words, at least some of the phases in the presumed source region would have had to crystallize from a liquid that already had very high REE concentrations, and there is no need to postulate a partial melting process to account for the presence of REE-rich liquids. Second, the few known samples of lunar rocks with high olivine contents are too low in bulk Fe/(Fe + Mg) to yield liquids similar to those of Fra Mauro basalts even at extremely small amounts of melting. Third, there is an apparent paradox in the plumbing system: a liquid in the source region would have to maintain contact with the residual phases long enough to reach equilibrium, yet the plumbing must be efficient enough to allow removal of a very small amount of liquid. Lastly, why would such a cumulate begin to melt in the first place?

Residual-liquid model

Estimates of bulk moon compositions have been used by many authors as the composition of the original lunar-wide magma. Two of the most popular are those by Ganapathy and Anders (1974) and Taylor and Jakeš (1974). Both compositions are reasonably close to composition *P* (Fig. 6) when projected onto the iron-41 plane, but have different Fe/(Fe + Mg) values (0.05 and 0.15 respectively). The projection of the equilibrium crystallization path of *P* would be *P–S–R–B* (Fig. 6). When the liquid reaches the (si) curve (Fig. 4), which projects at point *B* (Fig. 6), olivine starts to dissolve and orthopyroxene and anorthite crystallize until the liquid freezes. The liquid ends along the (si) curve, thus producing Fra Mauro basalts. However, the mineralogical variation of the highland rocks argues against equilibrium crystallization, which anyway could not produce liquids with high enough concentrations of incompatible elements. Thus equilibrium crystallization is not a realistic assumption in a very deep magma ocean, and fractional crystallization must be considered more likely. This is where the residual-liquid model runs into trouble. Despite the inadequacies of the partial-melting model, most authors prefer it over a residual-liquid origin for Fra Mauro basalt for the following reasons:

(1) A fractionally-crystallizing liquid starting out at *P* will eventually reach the olivine–orthopyroxene–anorthite "peritectic" but will have no tendency to remain at such a point. The liquid would move on to the orthopyroxene–anorthite–silica "eutectic," and it would be fortuitous for a liquid to be extracted at this transient point of the crystallization sequence (Walker *et al.*, 1972); (2) because of the very high REE content of Fra Mauro basalt, the very large amount of fractional crystallization (at least 90%) would result in prohibitively high Fe/(Fe + Mg) values of the residual liquid (Prinz *et al.*, 1973); (3) a fractionating liquid starting out with 7–10× chondritic REE abundances would develop Sm/Eu ratios which rise too steeply with increasing crystallization to be representative of Fra Mauro basalt trends (Weill *et al.*, 1974).

We will consider these objections in order:

(1) The experimental data presented here demonstrate that the olivine–orthopyroxene–anorthite point in the iron-41 plane is *not* a peritectic, but a piercing point created by a "quaternary" univariant curve

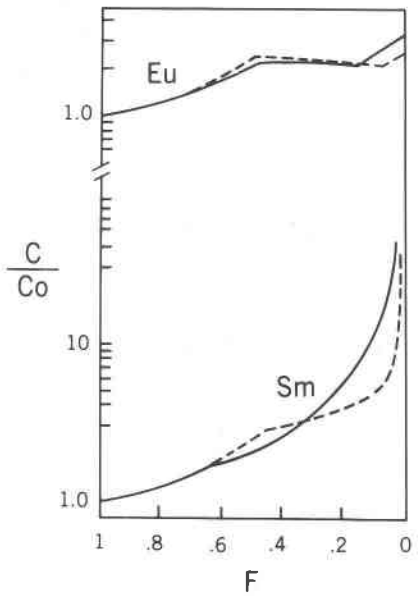

Fig. 8. The Sm/Eu evolution during fractional crystallization of liquids 2 (solid line) and *P* (broken line) from Fig. 6. The bulk compositions of the two liquids are shown in Fig. 6. *C* = concentration in residual liquid, *Co* = original concentration, *F* = wt. fraction of liquid remaining. Format and data are from Weill *et al.* (1974). For further explanation see text.

along which the three crystalline phases coexist over a wide range of temperatures and liquid compositions. If fractional crystallization of the magma ocean were perfect it would be true that the liquid would have no tendency to remain along the (si) curve. But because of stirring due to thermal convection and/or bombardment, perfect fractional crystallization, like perfect equilibrium crystallization, is not a realistic assumption in a very deep magma ocean. Note that along the olivine–anorthite surface (*R–B* in Fig. 6) olivine is *not* in reaction relation with the liquid, so that when the (si) curve is reached it is reasonable to expect olivine to still be in contact with the liquid. Wood (1975) argued that the magma ocean was well stirred. Depending on how vigorously the magma is convecting, the olivine could remain in contact with the liquid for some time, keeping the liquid along the (si) curve. Figure 4 shows that the (si) curve is approximately normal to the iron-41 plane, and liquids along that curve with variable Fe/(Fe + Mg) values would project near point *B* (Fig. 6). Even after olivine has left the assemblage, liquids along the anorthite–opx surface (on curve *A–B* in Fig. 4 for instance) would still project reasonably close to point *B* in Figure 6.

(2) One of the main differences between the compositions suggested by Ganapathy and Anders, and Taylor and Jakeš, is in the bulk Fe/(Fe + Mg) (0.05 and 0.15 respectively). Let us consider the Fe–Mg evolution of the Ganapathy-Anders liquid first: A liquid starting out at *P* will undergo 92% crystallization before it reaches the (si) curve (PB/AB = 0.92 in Fig. 6), and the amount of olivine *vs.* anorthite separated from it will be 73:27, so 67% olivine has crystallized if the amount of spinel is volumetrically insignificant. The composition of the first olivine to crystallize is Fo_{98}. If *all* the 67% olivine is immediately separated from the liquid and *all* of the olivine is Fo_{98}, the Fe/(Fe + Mg) value of the liquid after 92% crystallization is 0.67. For a similar liquid composition Drake (1976) calculated the range of olivine compositions to be Fo_{98}–Fo_{95}. The same calculation using a more realistic average olivine composition of $Fo_{96.5}$ yields a residual liquid of Fe/(Fe + Mg) =0.37. Equilibrium crystallization of the Ganapathy-Anders composition would yield a residual liquid of Fe/(Fe + Mg) $\simeq$ 0.1 after 92% crystallization. Therefore, a bulk composition at *P* (Fig. 6) with bulk Fe/(Fe + Mg) = 0.05 can yield liquids with Fe/(Fe +Mg) between 0.10 and 0.37.

If the bulk Fe/(Fe + Mg) is tripled to 0.15, in order to bring it in line with the Taylor-Jakeš estimate, the first olivine to crystallize will be Fo_{94}. The average olivine composition will be Fo_{88} after 92% crystallization. Under these conditions the residual liquid would have Fe/(Fe + Mg) = 0.79 and equilibrium crystallization would yield a residual liquid with Fe/(Fe + Mg) = 0.33.

It is therefore possible to have a liquid with Fe/(Fe + Mg) ranging from 0.1 to 0.8 depending upon the choice of starting composition and the efficiency of fractionation. Fra Mauro basalts have Fe/(Fe + Mg) values ranging from 0.35 to 0.6.

All of the above calculations were made assuming the olivine–anorthite surface and the (si) curve are normal to the iron-41 plane and using the experimentally derived $K_D$ol-liq = 0.33. The calculations give a range of possible residual liquid compositions and show that greater than 90% crystallization *need not* be accompanied by prohibitively high Fe/(Fe + Mg) values.

(3) Weill *et al.* (1974) calculated that a liquid with a composition of #2 (Fig. 6) would develop Sm/Eu ratios that are too high for Fra Mauro basalts after relatively small amounts of fractional crystallization. The same calculation has been carried out for liquid *P* (Fig. 8) with the same partition values used by Weill *et al.* (1974) for comparison.

Clearly the rise in the Sm/Eu ratio during frac-

tional crystallization of liquid *P* is not nearly as rapid as that for liquid 2. The difference in Sm–Eu concentration paths is due to the fact that the evolution for trace elements depends upon the compositions and relative amounts of phases being separated from the liquid. As before, the calculations were made assuming the (si) curve, the opx–an, and ol–an boundary surface are normal to the iron-41 plane. Also, as before, the effect of fractionation of a small amount of spinel was considered to be insignificant relative to the silicates. Newer crystal/liquid partition coefficients (Weill and McKay, 1975, and McKay and Weill, 1976a) will revise the absolute amounts of both elements upward but will not greatly alter their ratios in residual-liquid calculations.

Effects of pressure on CaO/Al_2O_3 ratio and Fe enrichment

The two initial magma compositions being considered have a CaO/Al_2O_3 molar ratio of 1.4–1.45, and so have a substantial $Ca(Mg,Fe)Si_2O_6$ component (see, for example, Hodges and Kushiro, 1974). Experimental studies on the Ganapathy-Anders composition (Hodges and Kushiro, 1974) and the Taylor-Jakeš composition (Ringwood, 1976) confirm that these liquids become saturated with respect to Ca-rich clinopyroxene near the solidus. If the lunar-wide magma, which is being displaced upward by a thickening cumulate pile, arrives at the 60–100 km level saturated with Ca-rich clinopyroxene, its CaO/Al_2O_3 ratio would be much too high for the Fra Mauro basalts (see Hodges and Kushiro, 1974). However, if Ca-rich clinopyroxene fractionates at high pressure the CaO/Al_2O_3 ratio of the evolving liquid would be *lowered.* Results of phase equilibria studies by Hodges and Kushiro (1974) and Ringwood (1976) show that clinopyroxene fractionation at depth is a good possibility in each of the two initial magma compositions, and the liquid may arrive at the 60–100 km level with a low CaO/Al_2O_3 ratio and thus be close to the olivine–anorthite–silica composition plane.

Another interesting consequence of a large pressure gradient is that the cumulates at the bottom of the ocean will have a higher value of Fe/(Fe + Mg) than was calculated from the low-pressure partition coefficient (Walker *et al.,* 1975). As the floor of the ocean rises, the gradient decreases and this effect will be reduced. With this mode of crystallization, iron enrichment of the liquid is delayed. If the delay of iron enrichment is 5% of crystallization then the liquid will not reach the Fe/(Fe + Mg) values calculated in the previous section until crystallization is about 97% complete.

It is important to note that the two mechanisms outlined here would certainly *not* be the only, perhaps not even the most important, processes in a fractionating magma ocean. But it is not the intent of this report to present and evaluate all possible combinations of processes in a magma ocean. The intent rather is to show that mechanisms exist that will tend to affect the chemistry of the residual liquid of the ocean in such a way that Fra Mauro basalt compositions can be approached. Let us now examine the evidence on the composition of the evolving magma ocean that can be obtained from a presumed cumulate of the ocean.

Evidence on residual liquid compositions from troctolite 76535

Gooley *et al.* (1974) first described troctolitic sample 76535 and interpreted it as a rock of "deep" crustal origin. Since then 76535 has become one of the most extensively studied of all the lunar samples. Petrographic observations (Gooley *et al.,* 1974; Dymek *et al.,* 1975), chemical studies (Haskin *et al.,* 1974), and isotopic measurements (Bogard *et al.,* 1975; Lugmair *et al.,* 1976; Papanastassiou and Wasserburg, 1976) have led to the conclusion that 76535 is a relatively undisturbed cumulate of the original magma ocean (Dymek *et al.,* 1975).

Haskin *et al.* (1974) attempted to estimate the trace-element composition of the parent liquid of 76535 by assuming that 16% trapped liquid is present. They obtained the pattern shown in Figure 9. Lugmair *et al.* (1975) argued that very little trapped liquid is present in 76535, and estimated that Sm in the parent liquid was 30–40 times the amount now present in the plagioclase of 76535. This yields a Sm concentration in the liquid of up to 180× that found in chondrites. If the amount of trapped liquid in the rock is 8% (or less) the calculations of Haskin *et al.* show that REE concentrations and abundance patterns (Fig. 9) for the liquid from which 76535 crystallized are similar to those of Fra Mauro basalts.

Dymek *et al.* (1975) argued that the Fe/(Fe + Mg) values of the olivine (0.127) and orthopyroxene (0.118) in 76535 reflect the Fe/(Fe + Mg) values of its parent liquid. The K_D values for olivine and orthopyroxene (0.33 and 0.30 respectively, this report) may then be used to calculate the Fe/(Fe + Mg) of the parent liquid. The liquid had Fe/(Fe + Mg) = 0.31. Thus, if 8% or less trapped liquid is present in 76535, a relatively low Fe/(Fe + Mg) liquid with a high

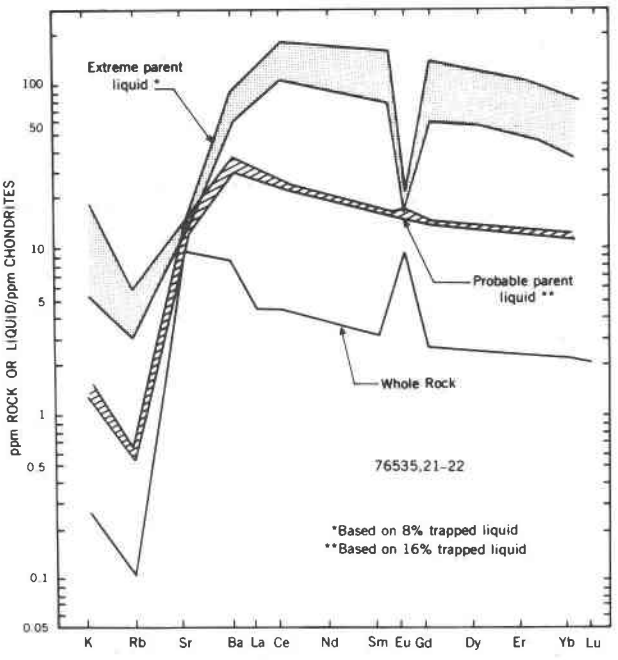

Fig. 9. A comparison of calculated parent liquid compositions of 76535 for 16% trapped liquid and 8% trapped liquid labelled "extreme parent liquid" as calculated by Haskin *et al.* (1974).

REE concentration and abundance pattern similar to Fra Mauro basalt evolved during fractionation of the lunar-wide magma.

Isotopic evidence

Rb–Sr systematics of Fra Mauro basalts have given us two different kinds of ages; internal isochrons (3.9–4.0 AE) and whole-rock isochrons (4.25–4.4 AE, Papanastassiou and Wasserburg, 1971; Wasserburg and Papanastassiou, 1971; Nyquist *et al.*, 1974, 1975). Shih (1976) obtained an average whole-rock isochron of 4.36 ± 0.03 AE. Ages obtained through U–Th–Pb systematics are usually discordant but intersect concordia at 4.4 and 3.9 AE (Nunes *et al.*, 1975; Tera and Wasserburg, 1974). Schonfeld and Meyer (1972), Nyquist *et al.* (1974, 1975), and Shih (1976) have used these data to suggest the Fra Mauro basalts were formed at 4.36 AE and were later subjected to metamorphism and/or melting due to heavy bombardment which rapidly subsided at 3.9–4.0 AE. Thus the younger ages probably represent total or partial resetting of the isotopic clocks without substantially opening the system. Corroborating evidence that Fra Mauro basalts are older than 3.9–4.0 AE is obtained from ^{39}Ar–^{40}Ar ages of highland breccias (Eberhardt *et al.*, 1976). The completion of the fractionation of the lunar-wide magma ocean has been indirectly dated at 4.35 AE using Nd–Sm systematics by Lugmair *et al.* (1975). Tera and Wasserburg (1974) indirectly dated the end of the fractionation process at 4.42 AE using U–Th–Pb. The average formation age of Fra Mauro basalts of 4.36 AE is remarkably close to the completion of the lunar-wide magma fractionation.

If equilibrium partial melting produced Fra Mauro basalts, isotopic fractionation would have occurred at the time of melting and the 4.3–4.4 AE ages would date the event. The similarity of the formation ages of Fra Mauro basalts and the completion of the fractionation process of lunar-wide magma ocean would then be coincidental. But if Fra Mauro basalts are residual liquids, the agreement between their formation ages and the end of the fractionation process is not coincidence, it is required.

Albee and Gancarz (1974) suggested that mare basalts might be the result of a fractional partial melting process involving mostly interstitial minor phases rich in the incompatible elements. In such a process mare basalts would not reflect the bulk major-element chemistry of the source. If such a process was responsible for the Fra Mauro basalts, it is highly unlikely that the resultant liquids would conform so well to the boundary curves in the olivine–anorthite–silica plane.

Conclusions

Most authors have favored partial melting over the simpler residual-liquid origin for Fra Mauro basalts, more because of the negative aspects of the residual-liquid model than the positive aspects of partial melting. The data presented here show that:

(1) It is possible, even probable, for residual liquids of a lunar-wide magma to remain in the vicinity of the (si) curve during crystallization.

(2) Unacceptably high Fe/(Fe + Mg) values need not accompany the very large amounts of fractionation required for the high trace-element concentrations.

(3) One of the few samples (76535) which lunar scientists believe might be an undisturbed cumulate of the magma ocean probably crystallized from a liquid with trace-element concentrations, abundance pattern, and major-element chemistry very similar to that of Fra Mauro basalts.

Some of the features that make the residual-liquid model attractive are:

(1) A heat source for a partial melting event at 4.3–4.4 AE is not required.

(2) The agreement between the formation ages of

Fra Mauro Basalts and the crustal differentiation age does not depend on coincidence.

Acknowledgments

The author thanks R. Brett, J. S. Huebner, M. Sato, D. Walker, and D. Wones for constructive discussions. The manuscript has benefited from careful reviews by R. Brett, R. Helz, J. S. Huebner, A. J. Irving, I. S. McCallum, R. B. Merrill, D. B. Stewart, D. Walker, and J. A. Wood. Thanks are also due to D. Walker and J. A. Wood for kindly providing the author with unpublished data. The work was performed during the author's NRC postdoctoral associateship at the U.S. Geological Survey. Partial support was provided by NASA contract 2356-A, J. S. Huebner, P. I.

References

The following abbreviations are used throughout:
PLC 2, 3, 4, 5, 6: Proceedings 2nd etc. Lunar Science Conference, Geochim. Cosmochim. Acta Suppl. 2, etc.

Albee, A. L. and A. L. Gancarz (1974) Petrogenesis of lunar rocks: Rb–Sr constraints and lack of H_2O. *Proc. Soviet-American Conf. Cosmochim. Moon and Planets*. Lunar Sci. Institute, Houston, 46–53.

Andersen, O. (1915) The system anorthite–forsterite–silica. *Am. J. Sci., 39,* 407–454.

Bogard, D. D., L. E. Nyquist, B. M. Bansal, H. Wiesmann, and C. Y. Shih (1975) 76535: an old lunar rock. *Earth Planet. Sci. Lett., 26,* 69–80.

Bowen, N. L. and J. F. Schairer (1935) The system MgO–FeO–SiO_2. *Am. J. Sci., 229,* 151–217.

Brett, R. (1977) The case against early melting of the bulk of the moon. *Geochim. Cosmochim. Acta, 41,* 443–445.

Dowty, E., K. Keil, M. Prinz, J. Gros and H. Takahashi (1976) Meteorite-free Apollo 15 crystalline KREEP. *PLC 7,* 1833–1844.

Drake, M. J. (1976) Evolution of major mineral compositions and trace element abundances during fractional crystallization of a model lunar composition. *Geochim. Cosmochim. Acta, 40,* 401–412.

Dymek, R. F., A. L. Albee and A. A. Chodos (1975) Comparative petrology of lunar cumulate rocks of possible primary origin: dunite 72415, troctolite 76535, norite 78235 and anorthosite 62237. *PLC 6,* 301–341.

Eberhardt, P., J. Geiss, N. Grögler, P. Maurer, A. Stettler, A. Peckett, G. M. Brown and U. Krähenbühl (1976) Young and old ages in the Descartes region. *Lunar Sci. VII,* 233–235. Lunar Sci. Institute, Houston.

Ganapathy, R. and E. Anders (1974) Bulk compositions of the moon and earth, estimated from meteorites. *PLC 5,* 1181–1206.

Gooley, R., R. Brett, J. Warner and J. R. Smyth (1974) A lunar rock of deep crustal origin: sample 76535. *Geochim. Cosmochim. Acta, 38,* 1329–1339.

Haskin, L. A., C. Y. Shih, B. M. Bansal, J. M. Rhodes, H. Wiesmann, and L. E. Nyquist (1974) Chemical evidence for the origin of 76535 as a cumulate. *PLC 5,* 1213–1225.

Hodges, F. N. and I. Kushiro (1974) Apollo 17 petrology and experimental determination of differentiation sequences in model moon compositions. *PLC 5,* 505–520.

Hubbard, N. J., P. W. Gast, J. M. Rhodes, B. M. Bansal, H. Wiesmann, and S. E. Church (1972) Non-mare basalts: Part II. *PLC 3,* 1161–1179.

———, J. M. Rhodes, H. Wiesmann, C. Y. Shih, and B. M. Bansal (1974) The chemical definition and interpretation of rock types returned from the non-mare regions of the moon. *PLC 5,* 1227–1246.

Lugmair, G. W., N. B. Scheinin and K. Marti (1975) Sm–Nd age and history of Apollo 17 basalt 75075: evidence for early differentiation of the lunar exterior. *PLC 6,* 1419–1429.

———, K. Marti, J. P. Kurtz and N. B. Scheinin (1976) History and genesis of lunar troctolite 76535 or: how old is old? *PLC 7,* 2009–2033.

McCallum, I. S. and E. A. Mathez (1975) Petrology of noritic cumulates and a partial melting model for the genesis of Fra Mauro basalts. *PLC 6,* 395–414.

McKay, G. A. and D. F. Weill (1976a) Application of major and trace element crystal/liquid partitioning to the origin of KREEP. *Lunar Sci. VII,* 527–529. Lunar Sci. Institute, Houston.

——— and ——— (1976b) Petrogenesis of KREEP. *PLC 7,* 2427–2447.

Muan, A. and J. F. Schairer (1971) Melting relations of materials of lunar compositions. *Carnegie Inst. Wash. Year Book, 69,* 243–245.

Nunes, P. D., M. Tatsumoto and D. M. Unruh (1975) U–Th–Pb systematics of anorthositic gabbros 78155 and 77017. *PLC 6,* 1431–1444.

Nyquist, L. E., B. M. Bansal, H. Wiesmann and B. M. Jahn (1974) Taurus-Littrow chronology: some constraints on early lunar crustal development. *PLC 5,* 1515–1539.

———, ——— and ——— (1975) Rb–Sr ages and initial $^{87}Sr/^{86}Sr$ for Apollo 17 basalts and KREEP basalt 15386. *PLC 6,* 1445–1465.

Papanastassiou, D. A. and G. J. Wasserburg (1971) Rb–Sr ages of igneous rocks from the Apollo 14 mission and the age of the Fra Mauro Formation. *Earth Planet. Sci. Lett., 12,* 36–48.

——— and ——— (1976) Rb–Sr age of troctolite 76535. *PLC 7,* 2035–2054.

Powell, B. N., M. A. Dungan and P. W. Weiblen (1975) Apollo 16 feldspathic melt rocks: clues to the magmatic history of the lunar crust. *PLC 6,* 415–433.

Prinz, M., E. Dowty, K. Keil and T. E. Bunch (1973) Mineralogy, petrology and chemistry of lithic fragments from Lunar 20 fines: origin of the cumulate ANT suite and its relationship to high-alumina and mare basalts. *Geochim. Cosmochim. Acta, 37,* 979–1006.

Reid, A. M., W. I. Ridley, R. S. Harmon, J. Warner, R. Brett, P. Jakeš and R. W. Brown (1972a) Highly aluminous glasses in lunar soils and the nature of the lunar highlands. *Geochim. Cosmochim. Acta, 36,* 903–912.

———, J. Warner, W. I. Ridley, D. A. Johnston, R. S. Harmon, P. Jakeš and R. W. Brown (1972b) The major element compositions of lunar rocks as inferred from glass compositions in the lunar soils. *PLC 3,* 363–378.

———, ———, ——— and R. W. Brown (1972c) Major element composition of glasses in three Apollo 15 soils. *Meteoritics, 7,* 395–415.

Rhodes, J. M. and N. J. Hubbard (1973) Chemistry, classification, and petrogenesis of Apollo 15 mare basalts. *PLC 4,* 1127–1148.

Ringwood, A. E. (1976) Limits on the bulk composition of the moon. *Icarus, 28,* 325–350.

Roedder, E. and P. W. Weiblen (1972) Occurrence of chromian, hercynitic spinel ("pleonaste") in Apollo-14 samples and its petrologic implications. *Earth Planet. Sci. Lett., 15,* 376–402.

Roeder, P. L. and E. F. Osborn (1966) Experimental data for the system MgO–FeO–Fe_2O_3–$CaAl_2Si_2O_8$–SiO_2 and their petrologic implications. *Am. J. Sci., 264,* 428–480.

Schonfeld, E. and C. Meyer Jr. (1972) The abundances of com-

ponents of the lunar soils by a least-squares mixing model and the formation age of KREEP. *PLC 3,* 1397–1420.

Shih, Chi-Yu (1976) The origin of KREEP basalt. *Lunar Sci. VII,* 800–802. Lunar Sci. Institute, Houston.

Taylor, S. R. (1975) *Lunar Science: A post-Apollo view.* Pergamon Press. New York.

——— and P. Jakeš (1974) The geochemical evolution of the moon. *PLC 5,* 1287–1305.

Tera, F. and G. J. Wasserburg (1974) U–Th–Pb systematics on lunar rocks and inferences about lunar evolution and the age of the moon. *PLC 5,* 1571–1599.

Walker, D., J. Longhi and J. F. Hays (1972) Experimental petrology and origin of Fra Mauro rocks and soil. *PLC 3,* 797–817.

———, T. L. Grove, J. Longhi, E. M. Stolper and J. F. Hays (1973) Origin of lunar feldspathic rocks. *Earth Planet. Sci. Lett., 20,* 325–336.

———, J. Longhi and J. F. Hays (1975) Differentiation of a very thick magma body and implications for the source regions of mare basalts. *PLC 6,* 1103–1120.

Wasserburg, G. J. and D. A. Papanastassiou (1971) Age of an Apollo 15 mare basalt: lunar crust and mantle evolution. *Earth Planet. Sci. Lett., 13,* 97–104.

Weill, D. F., G. A. McKay, S. J. Kridelbaugh and M. Grutzeck (1974) Modeling the evolution of Sm and Eu abundances during lunar igneous differentiation. *PLC 5,* 1337–1352.

——— and G. A. McKay (1975) The partitioning of Mg, Fe, Sr, Ce, Sm, Eu, and Yb in lunar igneous systems and a possible origin of KREEP by equilibrium partial melting. *PLC 6,* 1143–1158.

Wood, J. A. (1975) Lunar petrogenesis in a well-stirred magma ocean. *PLC 6,* 1087–1102.

Manuscript received, April 11, 1977; accepted for publication, October 13, 1977.